Modeling of Nano-Scale Electrokinetic Thrusters

IEPC-2011-235

Presented at the 32nd International Electric Propulsion Conference,
Wiesbaden • Germany
September 11 – 15, 2011

F. J. Diez[1], G. Hernaiz[2], J. J. Miranda[3]
Rutgers, The State University of New Jersey, Piscataway, NJ, 08854 USA

and

M. Sureda[4]
ETSEIAT, Universitat Politècnica Catalunya,Terrassa, Spain

Abstract: A theoretical analysis considering the capabilities of electrokinetic actuators in the field of space propulsion is presented. The work describes an electro-hydro-dynamic model of the electrokinetic flow in nano-channels and represents the first attempt to exploit the advantages of the electrokinetic effect as the basis for a new class of nano-scale thrusters suitable for space propulsion. Among such advantages are their small volume, fundamental simplicity, overall low mass, and actuation efficiency. The electrokinetic efficiency in nano-scale actuators is affected by the slip length, surface charge, pH and molarity. These design variables are analyzed and optimized for the highest electrokinetic performance inside nano-channels. The optimization is done for power consumption, thrust and specific impulse resulting in high theoretical efficiency ~99% with corresponding high thrust-to-power ratios. The end effects at the entrance and exit of the electrokinetic actuator are also discussed including a numerical simulation between the fluid reservoir and the nano-thruster. Performance curves are obtained for the electrokinetic design variables showing that high molarity electrolytes lead to high thrust and specific impulse values, whereas low molarities provide the highest thrust-to-power ratios and efficiencies. A theoretical case study from the optimized curves shows that a 100 nm wide and 1μm long electrokinetic emitter would deliver thrusts from 5 to 43 μN, specific impulse from 60 to 210s, and would have power consumption between 1-15 mW. By designing an array composed of thousands of these electrokinetic emitters, it would result in a flexible and scalable propulsion system capable of providing a wide range of thrust control for different mission scenarios and maintaining very high efficiencies and thrust-to-power ratio by varying the number of emitters in use at any one time.

Nomenclature

b	=	slip length
E_Z	=	electric field across the channel
e	=	positron charge
F_Z	=	electric body force
$g_1, \ldots g_5$	=	averaged integral functions
h	=	height of the square cross-sectional channel

[1] Associate Professor, Dept. Mechanical & Aerospace Eng., diez@rutgers.edu, corresponding author.
[2] Visiting Student, Dept. Mechanical & Aerospace Eng.
[3] Visiting Student, Dept. Mechanical & Aerospace Eng.
[4] Lecturer, Aerospace Dept.

I	=	total current
I_{sp}	=	specific impulse
k	=	Boltzmann constant
L	=	length of the channel
$\dot{m}$	=	mass flow rate
n	=	unit normal vector to the wall
n_i	=	ion distributions
n_0	=	bulk ion concentration
P_{in}	=	power consumption
T	=	temperature
Th	=	thrust
V	=	electric potential
v	=	velocity of the electroosmotic flow
v_m	=	average velocity of the electroosmotic flow
w	=	width of the channel
x, y, z	=	coordinates on the channel

Greek Symbols

χ_{ek}	=	electrokinetic efficiency
ε_o	=	electric permittivity of free space
ε_r	=	relative permittivity of the aqueous solution
η	=	viscosity of the aqueous solution
κ	=	inverse of the Debye length
μ_{EOF}	=	electroosmotic flow mobility
μ_+	=	positive ion electroosmotic mobility
μ_-	=	negative ion electroosmotic mobility
μ^*	=	ratio of ion mobility to the electroosmotic flow mobility
ρ	=	density of the electrolyte
ρ_e	=	net charge density inside the channel
σ	=	surface charge on the channel's wall
ψ	=	electric potential distribution across the channel
ψ_m	=	electric potential in the center of the channel
ζ	=	zeta potential

I. Introduction

In the design of any space mission, one of the key objectives is to fabricate a platform capable of providing the required performance while maintaining a minimal weight and power consumption. Since the amount of mass that a rocket booster can send into an initial orbit is limited by its operational capability, it is important to develop lighter subsystems to ensure mission criteria are satisfied in the most efficient manner possible. Another fundamental limitation of nearly every space mission is cost, which is again related to the total mass of the spacecraft[1]. The total cost of a space vehicle is also dependent upon the average and peak electrical power demands that the mission will entail[2].

In recent years, new space-related undertakings, such as the orbital corrections of small satellites and the precise control of spacecraft performing combined measurements [3], have created a demand for high precision, low thrust, and efficient space propulsion systems. Moreover, changes in space exploration are anticipated due to the ever-increasing accessibility and refinement of space technologies, with special emphasis placed upon the development of low-cost missions. Such requirements have created economic incentives to make the payloads of space vehicles both small and light-weight, encouraging the current, increasing trend toward the miniaturization of space components. This miniaturization has promoted the use of micro and nano-satellites, which integrate limited power generation capabilities, low power requirements and scaled-down propulsion systems that remain capable both of maintaining the space vehicle's orbit and/or performing attitude control maneuvers.

Electric propulsion EP as a technology has been known of and investigated since the 1960's, yet it has remained in slow development due to insufficient onboard electrical power amongst most existing spacecraft and perhaps even a reluctance by many mission planners to deviate from more entrenched propulsion systems[4]. EP utilizes an externally provided electric power source to accelerate a propellant, producing useful thrust[5]. This technology is inherently mass efficient and can accelerate the exhaust stream to very high speeds, provided a large enough potential drop is supplied. A large variety of EP techniques have already been designed, investigated and tested, and some of these have been used as a secondary and even primary propulsion system on a space platform[6,7,8]. The present work proposes within the field of electrostatic propulsion a novel method based on the electrokinetic principle.

The discovery of the electrokinetic phenomena dates to the nineteenth century, when it was first observed experimentally[9]. Recently, research in the field of electrokinetics has focused on areas such as biology[10,11] and electronic design[10], among others and it has shown to be well-suited for pumping of liquids for mixing and displacement of liquids at micro-scales. Moreover, recent studies have shown the potential for using the electrokinetic effect as a mechanism to efficiently convert mechanical work into electrical energy[12,13]. One of the most technologically promising phenomena in the field of electrokinetics is electro-osmosis, where a fluid moves through a non-conductive micro- or nano-channel under an applied electric field. Recent studies have estimated that the highest obtained efficiencies ranged from 0.1%[15,16,17,18] to 3%[12] with a theoretical maximum of less than 13%[13]. The efficiency can be further increased by applying a surface modification[14] to the walls of the nano-channels to allow hydrodynamic slip at the walls with maximum efficiency approaching 100%[12]. Furthermore increase in efficiency can be obtained by operating these thrusters in the vacuum of space where the existing end of the actuator is not exposed to a back pressure. This suggest that by carefully designing electrokinetic thrusters for high efficiencies, theoretically large thrust-to-power ratios could be obtained which are comparable or higher to those of current space thrusters, including ion thrusters, NSTAR, XIPS, HiPEP, FEEP[19,20,21,22].

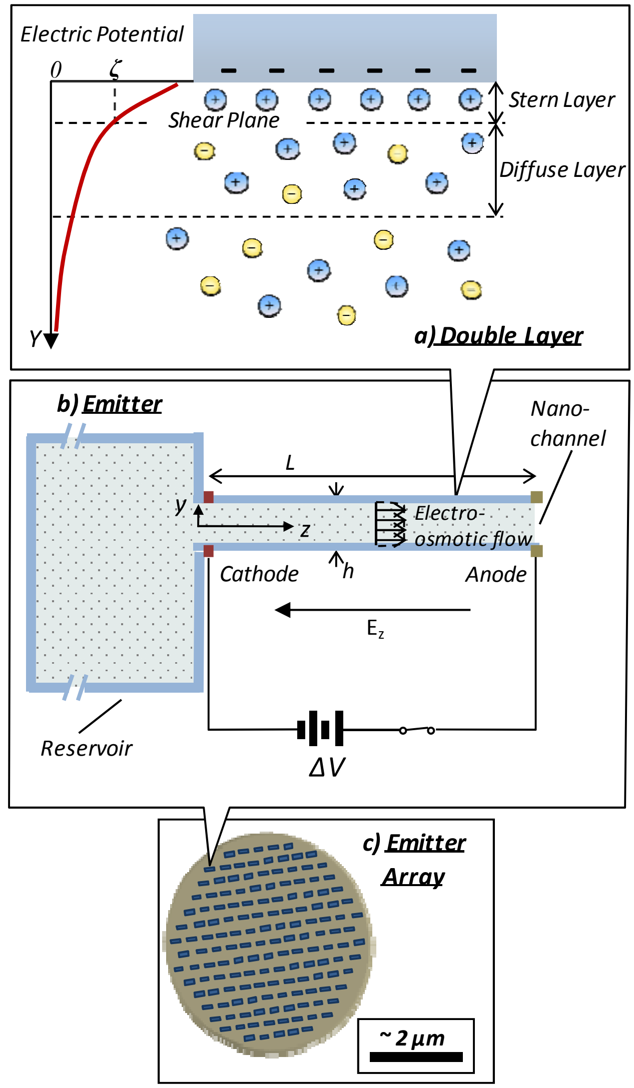

Fig. 1 *Schematic of electrokinetic thruster showing (a) typical ion distribution within electric double layer; (b) schematic of a single electrokinetic emitter showing the reservoir and its dimensions; (c) schematic of an array of 148 emitters.*

The present work proposes a new research area that bridges the gap between the established fields of micro/nano-fluidic electrokinetics and space propulsion to provide the basis for a new class of space micro-thrusters. The operating principle behind the proposed electrokinetic thrusters (ekT) exploits the nano-scale electric double layer that forms along non-conductive walls resulting in a stream of ions that can accelerate a column of a fluid when an electric potential across the non-conductive channel is applied. The paper starts with an electro-hydro-dynamic analysis of the electrokinetic flow in a nano-channel which will be optimized for space micro-thrusters. Next, the main electrokinetic design variables that affect the performance of the system are identified. The variables are then applied to a theoretical study of electrokinetic for space propulsion. Thrust, specific impulse and efficiency are the key parameters that are optimized in the analysis. Also, the expected performance characteristics of a designed ek emitter are presented and compared to other emitters.

II. Electro-hydro-dynamic Analysis

The electrokinetic effect arises from the interface between a dilute aqueous electrolyte solution and a non-conducting surface such as the walls of a micro or nano-channel which are made of materials such as a variety of polymers or glass. The physics at this interface are known to create an electrical potential at a shear plane in the fluid very close to the wall and a surface charge, σ, on the wall of the surface. The potential at the shear plane is called the zeta potential, ζ, and affects the distribution of ions within the solution as shown in Fig. 1a. The ions in the solution with opposite charge to the wall (the counter-ions) are attracted to the wall and the co-ions are repelled. This produces a region near the wall known as the electric double layer, EDL, with increased counter-ions and reduced co-ions as shown in Fig. 1a. When an electrolyte solution (even those with very low ionic concentration such as deionized water with a concentration of 10^{-7} mol/L) fills a channel, this redistribution of ions in turn produces a transverse electric field, establishing an ionic charge density gradient throughout the fluid. Applying an electric field across the length of the channel (Fig. 1b) results in an induced flow through the channel called the electroosmotic flow. To characterize the proposed ek thrusters first the electroosmotic flow needs to be well understood. The following section derives the fluid velocity.

First, the ion distribution in a channel needs to be model to describe the electroosmotic flow. Two assumptions are commonly applied. First, the wall of the channel is assumed to be a perfect electrical insulator. Second, the net lateral current is assumed to be zero[23]. Under these conditions, equilibrium is maintained between the ionic diffusion and the conduction current within the channel, and the Boltzmann distribution describe the net charge density, ρ_e, at any point in the fluid,

$$\rho_e = e(n_+ - n_-) = -2n_0 e \sinh\left(\frac{e\psi}{kT}\right) \tag{1}$$

To solve for ρ_e in Eq. (1) the potential distribution ψ must be calculated. As will be shown, the electric body force that drives the flow in the channel and generates the electroosmotic flow also depends on ψ.

A. Potential Distribution

The transverse electric field generated within the channel induces a potential distribution which can be quantified by the Poisson equation. By introducing the ionic charge density from the earlier assumptions, a Poisson-Boltzmann equation can be derived,

$$\frac{d^2\psi}{dy^2} = -\frac{\rho_e}{\varepsilon} = \frac{\kappa^2 kT}{e}\sinh\left(\frac{e\psi}{kT}\right) \tag{2}$$

where 1/κ is the Debye length (a measure of the EDL thickness) and is given by

$$1/\kappa = \sqrt{\frac{\varepsilon kT}{2n_0 e^2}} \tag{3}$$

Analytical solutions can be obtained for ψ from Eq. (2) and they strongly depend on the characteristics of the electric double layer, EDL. In turn, the EDL thickness is dependent on the molarity of the fluid solution. For instance, when the bulk ionic concentration increases, more counter-ions are attracted close to the charged surface in order to reach the equilibrium resulting in a smaller EDL as described by Eq. (3). When calculating the thickness of the EDL two limits can be observed, one is given when the EDL is small compared to the size of the channel, and the other when the EDL occupies most of the channel and overlaps[23,24]. Therefore, the potential distribution solution depends on whether or not the EDL is overlapped. The variation between these distributions is defined by the electrokinetic radius, κh/2, where h is the height of the square cross-sectional channel.

As long as the electrokinetic radius is greater than 2, the EDL does not overlap or weakly overlaps. The potential distribution in this case is given by[25]

$$\psi = \frac{4kT}{e}\left[\left(\operatorname{artanh}\left(\tanh\left(\frac{e\zeta}{4kT}\right)\exp(-\kappa y)\right)\right) + \left(\operatorname{artanh}\left(\tanh\left(\frac{e\zeta}{4kT}\right)\exp(-\kappa(h-y))\right)\right)\right] \tag{4}$$

Here, the zeta potential, ζ, is a function of the fluid properties, including the solution's molarity and pH. Both ζ and the surface charge σ can be calculated from[26] when the EDL does not overlap. In case of overlap σ can be calculated according to[27]. When the electrokinetic radius is less than 2, the electric double layer overlaps, and the potential distribution is given by Behrens, S. H. *et al.* (1999)[28].

Typical solutions for the potential distribution are shown in Fig. 2 for three different molarities of 10^{-1}M, 10^{-3}M, and 10^{-5}M. The EDL does not overlap or weakly overlaps for 10^{-1}M and 10^{-3}M, resulting in an almost zero potential at the center of the channel and Eq. (4) is used. The EDL strongly overlaps for 10^{-5}M and an elliptic integral[28] is used to calculate that potential distribution.

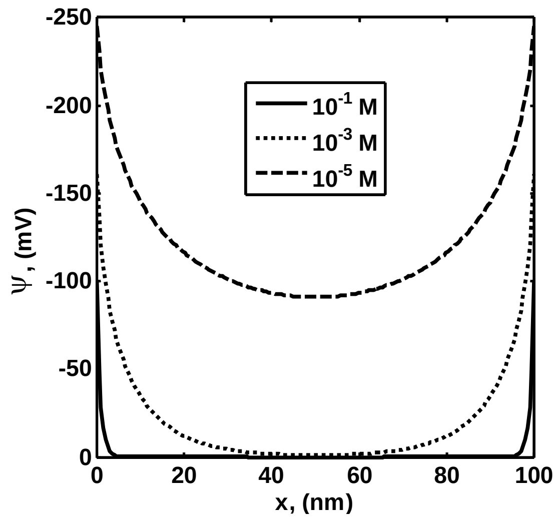

Fig. 2 *Electric potential across the width of a 100nm channel for three different molarities at constant pH of 9.*

B. Electroosmotic Flow

The electric body force in electroosmotic flows is just a Coulombic force given by

$$F_z = \rho_e E_z \tag{5}$$

which drives the flow in the channel. Together with the momentum equation, the Coulombic force can be used to solve for the velocity an the electrokinetic thrust. The resulting velocity profile is[12],

$$v = -\frac{\varepsilon\zeta}{\eta}\left[\left(1-\frac{\psi(y)}{\zeta}\right)-\frac{b}{\zeta}\left(\frac{-\sigma}{\varepsilon}\right)\right]E_z \tag{6}$$

where the first term on the right-hand side of the equation is called the electro-osmotic mobility ($\mu_{EOF} = \varepsilon\varsigma/\eta$). The velocity equation shows that the two physical effects driving the flow are the transversal electric field and the slip velocity at the channel wall. A representation of the velocity profile across the channel is shown in Fig. 3 where these two effects are considered in more detail. Figure 3 compares the velocity profiles in a 100 nm square channel (flow is considered 2D everywhere in this work for simplicity) for a constant value of the pH of 9 and a slip length of 20 nm, which results in increasing values of the surface charge for increasing values of the molarity with the resulting increase in velocity.

According to the previous analysis, it's clear that the surface charge and the slip condition will be two of the electrokinetic design parameters that can be used to control the velocity. The first depends on the solution properties (molarity and pH) and the second depends on the material of the channel and its surface treatment. The electric field is the third variable that can be used to regulate the velocity. This is the real control variable of the system, which can be regulated by varying the voltage applied across the channel.

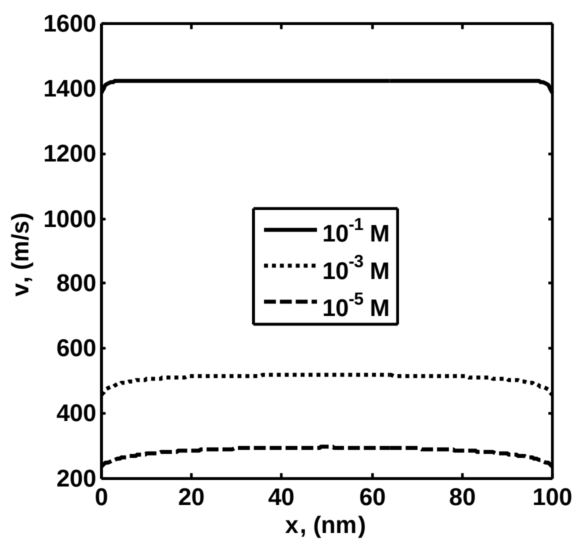

Fig. 3 *Calculated velocity profile across the width of a 100nm channel for three different molarities at constant pH of 9 for a slip length b = 20nm.*

The average electroosmotic flow velocity v_m can be obtained by integrating the velocity profile over the entire channel

$$v_m = -\frac{\varepsilon E_z \zeta}{\eta}\left(g_1 - \frac{b}{\zeta}\left(\frac{-\sigma}{\varepsilon}\right)\right) \tag{7}$$

where g_1 is the dimensionless value of the integral

$$g_1 = \frac{1}{h}\int\left(1-\frac{\psi}{\zeta}\right)dy \tag{8}$$

This expression of the velocity will be used in the propulsive analysis to determine the specific impulse, thrust, power and efficiency of the ekT.

III. Electrokinetic Propulsion Analysis

The previous electro-hydro-dynamic analysis is used to model the performance of an electrokinetic actuator as an emitter for space propulsion. This includes evaluating its thrust capabilities, specific impulse and efficiency. The dependence of these variables with the main electrokinetic parameters are also discussed. Considering that end effects can be significant in the operation of electrokinetic thrusters, a discussion of the entrance (exit) effects to (from) the nano-channel has been left for the Appendix including a numerical simulation of the flow between the reservoir and at the nano-channel (no analytical solution is possible in that region).

All the analytical calculations are obtained for the rectangular emitter sketched in Fig. 1b, with w = h = 100 nm and L = 1 μm. The applied electric field is $5{\cdot}10^8$ V/m which corresponds to a voltage drop between the electrodes of 500 V. Electric field values as high as $5\text{-}7{\cdot}10^8$ V/m have been used in molecular dynamic simulations of electro-osmotic flows for water solutions[31], although lower electric breakdown values for water have also been reported[32]. The applied ΔV can be easily reached by the propulsion power units (PPU) used in current space thrusters.

A. Thrust

Thrust is achieved by the electroosmotic effect in the nano-channel by transforming the input electrical power to total kinetic power. During typical operation, thrust levels will be controlled by the applied voltage across the nano-channel. The thrust developed by an ek emitter is proportional to the exhaust velocity and mass flow rate of the fluid, $Th = \dot{m}v$. Writing the mass flow rate ($\dot{m} = \rho v_m h w$) in terms of the electrokinetic variables and substituting it into the thrust equation gives the thrust developed by the emitter as a function of the electrokinetic design parameters,

$$Th = \rho w h\left(\frac{\varepsilon E_z \zeta}{\eta}\right)^2\left(g_1 - \frac{b}{\zeta}\left(\frac{-\sigma}{\varepsilon}\right)\right)^2 \tag{9}$$

Equation (9) is plotted in Fig. 4 and it shows the variation of thrust with surface charge density σ for several values of slip length b and a constant molarity of 10^{-1} M. The figure shows that the thrust increased with σ, resulting in values as high as 30 μN for the modeled emitter. Considering the nano-scale size of each emitter, an array could be designed with thousands of emitters working at low thrust levels for high-precision space propulsion systems.

Figure 4 also shows that increasing the slip length results in a significant increase on the thrust values and that for a fixed slip length b the thrust increases with σ. In fact, for any given combination of molarity and σ, an optimal slip length b can be found such that thrust is maximized. It should be noted that slip lengths greater

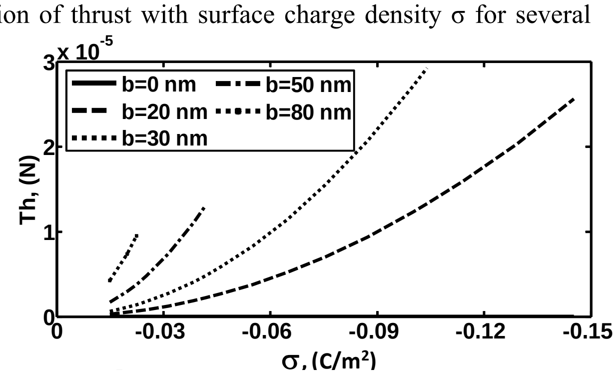

Fig. 4 *Thrust generated by a 100nm emitter for different slip lengths and for a molarity of 10^{-1}M*

than 30 nm are incompatible with a wide range of σ. At present, these effects are not well known, but some studies have concluded that they are related to a competition between the efficiency gains from advecting more counter-ions in the double layer as σ increases and the increased resistive dissipation caused by the additional counter-ions[12]. Taking this into consideration, a maximum value of b = 30 nm will be used as the reference to obtain the ek emitter performance value from Fig. 4 as follows: Th = 30 μN for a molarity of 10^{-1} M and σ = -0.105 C/m2, with a specific impulse Isp in the hundreds of seconds with a more detail analysis of the Isp done in sec. III.B and sec. IV.

B. Efficiency

One of the most important considerations for electric space propulsion systems is to have high efficiency. To fully characterize the efficiency of ekT, the critical role that the slip length and the electrolyte solution properties play on the optimization of ekT performances is considered through a parametric study. The electrokinetic efficiency is defined as the ratio of the ekT power output to the electrokinetic power input, and it is obtained from the classical expression for efficiency

$$\chi_{ek} = \frac{P_{out}}{P_{in}} = \frac{\dot{m} v_m^{\ 2}}{2 I \Delta V} \tag{10}$$

The ekT power output is the kinetic energy per unit time and both v_m and $\dot{m}$ can be written in terms of the electrokinetic variables using Eq. (7). Similarly the power input can also be derived. Thus, the efficiency can be rewritten as

$$\chi_{ek} = \frac{\rho}{4} \frac{\left(\frac{\varepsilon\zeta}{\eta}\right)^2}{e n_0} \left[\frac{\left(g_1 - \frac{b}{\zeta}\left(\frac{-\sigma}{\varepsilon}\right)\right)^3}{g_2 \mu^* + \left(g_3 - g_4 \frac{b}{\zeta}\left(\frac{-\sigma}{\varepsilon}\right)\right)} \right] \frac{E_z}{L} \tag{11}$$

The terms g_2, g_3, and g_4 are introduced to simplify the expression and correspond to the average values obtained after integrating the following expressions

$$g_2 = \frac{1}{h}\int_h \cosh\left(\frac{e\psi}{kT}\right) dh \tag{12}$$

$$g_3 = \frac{1}{h}\int_h \sinh\left(\frac{e\psi}{kT}\right)\left(1 - \frac{\psi}{\zeta}\right) dh \tag{13}$$

$$g_4 = \frac{1}{h}\int_h \sinh\left(\frac{e\psi}{kT}\right) dh \tag{14}$$

Defined this way, the efficiency is only related to the electrokinetic process in the micro/nano-channel and it does not take into account PPU consumption and other inefficiencies. However, nothing suggests that these factors should be bigger than those of existing EP systems which estimate internal thruster efficiency by multiplying by $\chi_{loss} \approx 0.95$.

The efficiency is plotted in Fig. 5 for a molarity of 10^{-1} M using the proposed electrokinetic model from Eq. (11). The plot takes into account five different slip lengths b, and shows that χ_{ek} increased with the surface charge σ and with b. For instance, if $b \sim 30$ nm the efficiency reaches 99%. Such high values exceed those achieved by major state-of-the-art EP systems, proving the large potential of electrokinetic thrusters as a space propulsion system when high efficiency is a main requirement. The high slope of the curves in Fig. 5 shows that the electrokinetic

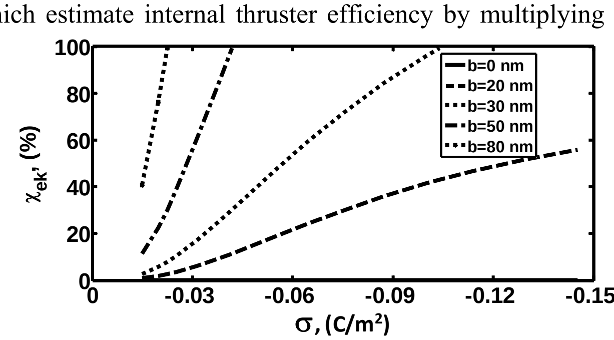

Fig. 5 *Calculated electrokinetic efficiency for a 100nm emitter for different slip lengths and for a molarity of 10^{-1} M*

efficiency is very sensitive to σ variations, especially for high values of *b*. This implies great precision needed when adjusting the ek parameters to obtain the highest efficiency for a given ekT design. In practice, achieving high slip lengths through surface modifications is still a topic of intense research, but still efficiencies over 99% can be obtained for more moderate slip lengths (20-40 nm) for the modeled 100 nm ek emitter used for the calculations in Fig. 5.

C. Thrust-to-Power Ratio

Another key parameter in the design of space propulsion systems is the thrust-to-power ratio which can be written for electrokinetic emitters

$$\frac{Th}{P_{in}} = \frac{\rho}{2} \frac{\left(\frac{\varepsilon\zeta}{\eta}\right)}{en_0} \left[\frac{\left(g_1 - \frac{b}{\zeta}\left(\frac{-\sigma}{\varepsilon}\right)\right)^2}{g_2\mu^* + \left(g_3 - g_4\frac{b}{\zeta}\left(\frac{-\sigma}{\varepsilon}\right)\right)} \right] \frac{1}{L} \tag{15}$$

This ratio strongly impacts major space mission's characteristics such as duration of thrust, system cost and payload capability. In order to show the propulsion capabilities of the ekT, the thrust-to-power ratio is calculated as a function of the specific impulse I_{sp} in Fig. 6. These Th/P_{in} results correspond to a constant potential drop of 500 V, and optimal ek parameters resulting in χ_{ek} close to 100%. Figure 6 shows that high molarities lead to high thrust and specific impulse values, whereas low molarities are needed in order to obtain higher thrust-to-power-in ratios for the highest efficiencies.

IV. Performance and Design

The previous results show the importance of electrokinetic parameters such as molarity, surface charge density and slip length, for optimum design conditions for specific space propulsion missions. Although it is not possible to directly vary these parameters during mission operation they can be chosen during the design and fabrication of the ek emitters. This can be achieved by optimal selection of actuator fabrication material, actuator dimensions and electrolyte solution in order to get *σ* and *b* for maximum electrokinetic efficiency.

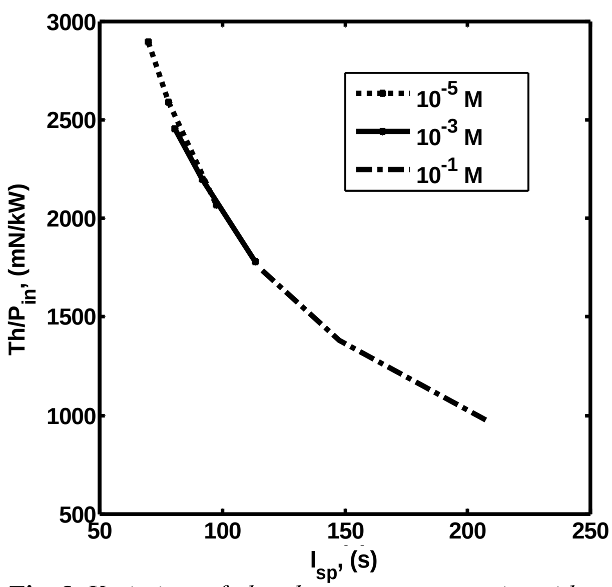

Fig. 6 *Variation of the thrust-to-power ratio with specific impulse for a 100nm emitter for three different molarities. Values shown correspond to optimal design electrokinetic variables (b, σ) with 100% efficiencies.*

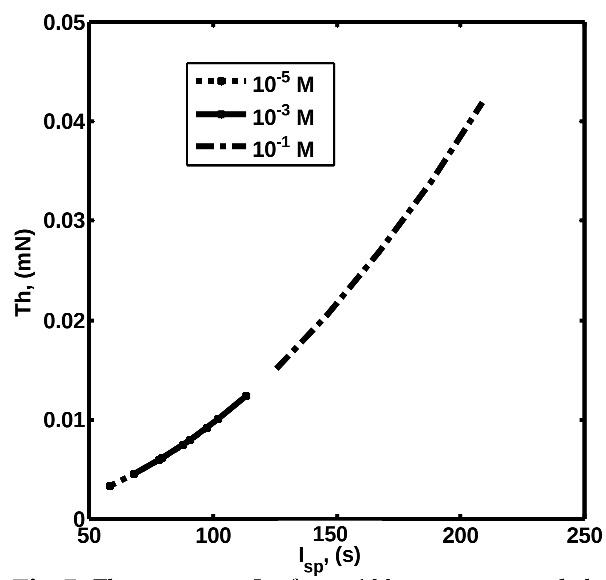

Fig. 7 *Thrust versus I_{sp} for a 100nm emitter and three different molarities. The plot shows the effects of externally controlling the electric potential drop such that for each molarity the lowest I_{sp} corresponds to 300V potential drop and the highest corresponds to 500V.*

What can be varied during mission operation is the total potential drop, ΔV, which allows direct control of the thrust and specific impulse of the ek emitter while thrust-to-power ratio remains constant for all ΔV values. If more thrust or higher thrust control is required than the one provided by a single emitter, an array with large number of emitters can be constructed. This would allow varying thrust levels incrementally while maintaining efficiency and specific impulse at their optimal values by simply varying the number of emitters in use at any one time.

The thrust capabilities of a single rectangular emitter, such as the one sketched in Fig. 1b, with $w = h = 100$ nm and $L = 1$ μm, are shown in Fig. 7. In this figure both the thrust and the I_{sp} increase by simply increasing the potential drop from 300 V to 500 V. Each curve in Fig. 7 represents a different molarity and the electrokinetic parameters for each one of these curves are selected to ensure close to 100% efficiency. The derived electrokinetic parameters for Fig. 7 are: (1) molarity of 10^{-1}M with $b = 27$ nm and $\sigma = -138.6$ mC/m^2, (2) molarity of 10^{-3}M with a $b = 34$ nm and $\sigma = -58$ mC/m^2, and (3) molarity of 10^{-5}M with $b = 37$ nm and $\sigma = -45.2$ mC/m^2. In terms of performance, Fig. 7 shows that the designed single ek emitter can deliver a thrust from 5 to 43 μN and a I_{sp} from 60 to 210 s**.** To cover the entire range of thrust operation shown in Fig. 7, it would require a system that would change the molarity on the fly by loading the solute and the solution separately to prepare the mixture in situ.

Considering that ekT are easily scalable, another alternative is developing an array composed of thousands of emitters to provide a wide range of thrusts for different mission scenarios with very high efficiencies and very high thrust control.

A comparison of the ek thrusters with other electric propulsion systems[2,33,34,20], is shown in Fig. 8. It compares the thrust-to-power ratio for a variety of EP systems as well as for two modeled ek thrusters. Full details for the two ekT are shown in Table 1. For both configurations, varying the potential from 300 V to 500 V increases the thrust and specific impulse but the thrust-to-power ratio remains constant. Also, the electro-hydro-dynamic analysis indicates that the two configurations are capable of delivering thrust with efficiency close to 100%. The comparison in Fig. 8 of colloidal thrusters with ek thrusters shows that they could be used for a similar Th and I_{sp} operation range but in a more efficient manner.

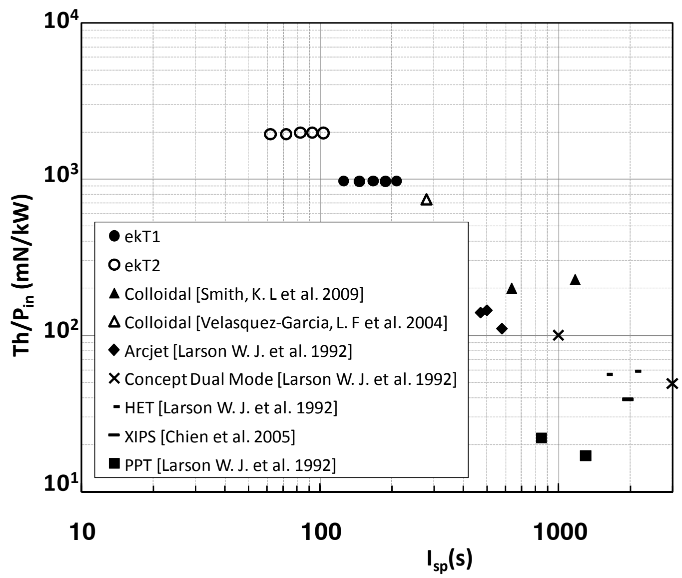

Fig. 8 *Thrust-to-power ratio and I_{sp} for different EP systems including the expected performance of the two designed (Table 1) ek emitter arrays.*

V. Conclusion

This work has demonstrated that the electrokinetic principle can provide the basis for a new class of space propulsion thrusters. The thrust is achieved by the electroosmotic effect in nano-channels by transforming input electrical power to total kinetic power. Specific performance characteristics for ek emitters for space propulsion have been determined from fundamental scaling laws for electrokinetic flows. This involved an electro-hydro-dynamic analysis based on the study of the electrokinetic flow in a nano-channel. The main electrokinetic parameters that affect the performance of the system are related to surface properties of the nano-channel and the electrolyte solution used. These electrokinetic design variables included the slip length, surface charge, pH and molarity. These variables were analyzed (for a fixed nano-channel length and width) to show, among other things, that designing ek emitters with increased surface charge density, and slip length all result in increases in velocity and I_{sp}.

The electrokinetic design variables were applied to the electrokinetic propulsion analysis. Thrust, specific impulse and efficiency were the key parameters considered in the analysis. One of the main strengths of the proposed electrokinetic thrusters for space applications is their high theoretical efficiency (90-100%) which results in high thrust-to-power ratios. Theoretical analysis showed that for all molarities considered the χ_{ek} increased with σ and with b. The evaluation of the χ_{ek} for electrokinetic emitters under optimal design conditions for highest electrokinetic efficiency showed that high molarity electrolytes can lead to high thrust and specific impulse values, whereas low molarities are needed in order to obtain higher thrust-to-power ratios for the highest efficiencies.

During typical operation, thrust levels would be dictated by the electrolyte solution properties and by the strength of the electric field which is the result of the applied voltage across the nano-channel. A maximum potential drop of 500 V was considered. Theoretical analysis showed that a single 100 nm wide and 1μm long ekT designed for maximum efficiency can deliver thrusts from 5 to 43 μN and a I_{sp} from 60 to 210 s. By designing an array composed of thousands of these electrokinetic emitters, it would result in a flexible and scalable propulsion system capable of providing a wide range of thrust control for different mission scenarios and maintaining very high efficiencies by varying the number of emitters in use at any one time.

Acknowledgments

The work presented was funded in part by the Office of Naval Research (N000141110019 managed by Dr. Thomas F. Swean)

References

[1]Wertz, J. R., and Larson, W. J., *Reducing Space Mission Cost*, Microcosm Press, El Segundo, CA, 1996.

[2]Larson W. J., and Wertz J. R., *Space Mission Analysis and Design*, Microcosm Press, El Segundo, CA, 1999.

[3]Smith, R. S., "Control of Deep-Space Formation-Flying Spacecraft; Relative Sensing and Switched Information," *Journal of Guidance, Control, and Dynamics*, Vol. 28, No. 1, Jan.–Febr. 2005, pp. 106-114.

[4]Martinez-Sanchez, M., and Pollard, J. E., "Spacecraft Electrical Propulsion – An Overview," *Journal of Propulsion and Power*, Vol. 14, No. 5, Sept.–Oct. 1998, pp. 688-699.

[5]Filliben, J. D., "Electric Thruster Systems," Chemical Propulsion Information Agency Rept. CPTR 97-65, June 1997.

[6]Sovey, J., Rawlin, V., and Patterson, M., "Ion Propulsion Development Projects in U.S.: Space Electric Rocket Test I to Deep Space I," *Journal of Propulsion and Power*, Vol. 17, No. 3, May-June 2001, pp. 517-526.

[7]Saccoccia, G., "European Activities in Electric Propulsion," Proceedings of the 3rd International Conference on Spacecraft Propulsion, Cannes, France, 2000.

[8]Toki, K., Kuninaka, H., Funaki, I., Nishiyama, K. and Shimizu, Y., "Development Status of a Microwave Ion Engine System for the Muses-C Mission," Proceedings of the 26th International Electric Propulsion Conference, Kitakyushu, Japan, 1999.

[9]Reuss, F. F., Memoires de la Societe Imperiale de Naturalistes de Moscou, Vol. 2, 1809, p. 327

[10]Chen, C. H., Zeng, S., Mikkelsen, J. C., and Santiago, J. G., "Development of a planar electrokinetic micropump," Proceedings of ASME 2000, MEMS 1, pp. 523–528, Orlando, USA, Nov. 5–10, 2000.

[11]Anderson, G. P., King, K. D., Cuttino, D. S., Whelan, J. P., Ligler, F. S., MacKrell, J. F., Bovais, C. S., Indyke, D. K., and Foch, R. J., "Biological agent detection with the use of an airborne biosensor," *Field Analytical Chemistry and Technology*, Vol 3, 1999, pp. 307-314.

[12]Ren, Y., and Stein, D., "Slip-enhanced electrokinetic energy conversion in nanofluidic channels," *Nanotechnology*, Vol. 19, No. 19, May 2008.

[13]Van der Heyden, F. H. J., Douwe, J. B., Derek, S., Christine, M., and Cees, D., "Electrokinetic Energy Conversion Efficiency in Nanofluidic Channels," *Nano Letters*, 6, No. 10, 2006, pp 2232-2237.

[14]Tretheway D. C., Meinhart C. D., "Apparent fluid slip at hydrophobic microchannel walls," *Physics of Fluids*, Vol. 14, No. 3, March 2002.

[15]Osterle, J. F., "Elctrokinetic Energy Conversion," *J. Appl. Mech.*, 1964, 31, pp. 161-164.

[16]Yang, J., Lu, F., Kostiuk, L. W., and Kwok, D. Y. J., "Electrokinetic microchannel battery by means of electrokinetic and microfluidic phenomena," *Journal of Micromechanics and Microengineering*, Vol. 13, No. 6, 2003, pp. 963-970.

[17]Olthuis, W., Schippers, B., and Eijkel, J.; van den Berg, A. "Energy from streaming current and potential," *Sensors and Actuators*, B 111, 2005, pp. 385-389.

[18]Chun, M.-S., Lee, T. S., and Choi, N. W., "Microfluidic analysis of electrokinetic streaming potential induced by microflows of monovalent electrolyte solution," *Journal of Micromechanics and Microengineering*, Vol. 15, No. 4, Feb. 2005, pp. 710-719.

[19]Brophy, J. R., Kakuda, R. Y., Polk, J. E., Anderson, J. R., Sovey, J., Patterson, M., Bond, T., Christensen, J., Matranga, M., and Bushway, D., "Ion Propulsion System (NSTAR) DS1 technology validation report," Deep Space 1 technology validation reports (A01-26126 06-12), Pasadena, CA, Jet Propulsion Laboratory, 2000.

[20]Chien, K. R., Tighe, W. G., Hart, S., De Pano, M. K., Bond, T. A., and Spears, R., "L-3 Communications ETI Electric Propulsion Overview," 29th International Electric Propulsion Conference, IEPC-2005-315, Princeton, New Jersey, Oct. 31 – Nov. 4, 2005.

[21]Oh, D. Y., "Evaluation of Solar Electric Propulsion Technologies for Discovery Class Missions," 41st AIAA/ASME/SAE/ASEE Joint Propulsion Conference & Exhibit, Tucson, Arizona, July 10 – 13, 2005.

[22]Liu, T. M., Musinski, L. D., Patel, P. R., Gallimore, A. D., Gilchrist, B. E., and Keidar, M., "Nanoparticle Electric Propulsion for Space Exploration," Space Technology and Applications International Forum-STAIF, Albuquerque, NM, Feb. 11-15, 2007.
[23] Burgreen, D., and Nakache, F. R., "Electrokinetic Flow in Ultrafine Capillary Slits," *Journal of Physical Chemistry*, 68, No. 5, Jan. 1964, pp. 1084–1091.
[24]Dongqing, L., *Electrokinetics in Microfluidics Vol. 2*, Elsevier, 2004
[25]García, A.L., Ista, L. K., Petsev, D. N., O'Brien, M. J., Bisong, P., Mammoli, A. A., Brueck, S. R., and López, G. P., **"**Electrokinetic molecular separation in nanoscale fluidic channels," *Lab. On a Chip*, 5, 2005, pp. 1271–1276.
[26]Behrens S. H., and Grier D. G., "The charge of glass and silica surfaces," *J. Chem. Phys.* Vol. 115 No. 14, 2001, pp. 6716-6721.
[27]Van der Heyden F., Stein D., and Dekker C., "Streaming currents in a single nanofluidic channel," *Phys. Rev. Lett.* Vol. 95 2005, 116104.
[28]Behrens, S. H., and Borkovec, M., "Electrostatic Interaction of Colloidal Surfaces with Variable Charge," *Journal of Physical Chemistry*, B, 1999, 103 (15), March 1999, pp. 2918–2928.
[29]Min, J. Y., Hasselbrink, E. F., and Kim, S. J., "On the efficiency of electrokinetic pumping of liquids through nanoscale channels," *Sensors and Actuators B: Chemical*, 98, No. 2, 2004, pp. 368 – 377.
[30]Rice, C. L., and Whitehead, R., "Electrokinetic flow in a narrow cylindrical capillary," *J. Physical Chemistry*, 69, No. 11, 1965, pp. 4017–4024.
[31]Joseph, S., and Aluru, N. R., "Hierarchical Multiscale Simulation of Electrokinetic Transport in Silica Nanochannels at the Point of Zero Charge," *Langmuir*, 22, No. 21, 2006, pp. 9041-9051.
[32]Kolb, J. F., Joshi, R. P., Xiao, S., and Schoenbach, K. H., "Streamers in water and other dielectric liquids," *Journal of Physics D: Applied Physics*, Vol. 41, No. 23, 2008.
[33]Smith, K. L., Stark, J. P., Krpoun, R., and Shea, H., "Performance of micro-fabricated Colloid thruster system," 31st International Electric Propulsion Conference, University of Michigan, Ann Arbor, Michigan, EEUU, Sept. 20 - 24, 2009.
[34]Velasquez, L. F., Akinwande, A. I., Martinez-Sanchez, M., "Advances in micro-fabricated droplet emission mode 1D colloid thruster array," 4th International Spacecraft Propulsion Conference (ESA SP-555), Chia Laguna (Cagliari), Sardinia, Italy, June 2 - 9, 2004.
[35]Yang, R.-J., Tseng, T.-I., Chang, C.-C., "End effects on electro-osmotic flows in micro-channels", *Journal of Micromechanics and Microengineering*, Vol. 15 ,2005, pp. 254–262.
[36]Karniadakis, G., Beskok, A., Aluru, N., "Microflows and nanoflows, Fundamentals and simulation", Springer, 2005.
[37]Baldessari, F., "Electrokinetics in nanochannels: Part I. Electric double layer overlap and channel-to-well equilibrium", *Journal Colloid Interface Science,* Vol. 325, No. 2, 2008, pp. 526–538.